Structural Characteristics of a 0.23 Mole Fraction Aqueous Solution of Tetrahydrofuran at 20 °C

Daniel T. Bowron,*,†,‡ John L. Finney,‡ and Alan K. Soper†,‡

ISIS Facility, CCLRC Rutherford Appleton Laboratory, Chilton, Didcot, Oxon OX11 0QX, U.K., and Department of Physics and Astronomy, University College London, Gower Street, London WC1E 6BT, U.K.

Received: July 3, 2006; In Final Form: August 11, 2006

Hydrogen/deuterium isotopic substitution neutron diffraction techniques were used to measure the structural correlation functions in a 0.23 mole fraction solution of tetrahydrofuran in water at room temperature. Empirical potential structure refinement (EPSR) was used to build a three-dimensional model of the liquid structure that is consistent with the experimental data. Detailed analysis shows a preference for nonpolar interactions between the cyclic ether molecules plus polar interactions between the ether and solvent water and hydrophobic hydration of the nonpolar regions of the solute. The increase in the number of hydrogen-bond-acceptor sites relative to the number of hydrogen-bond-donor sites in this system, compared to the balanced situation that would be found in pure water, has a marked compressive effect on the structure of the solvent. Despite the small size of the solvent water molecules, the 0.23 mole fraction aqueous solution is still found to contain small voids akin to those in pure liquid tetrahydrofuran. In contrast to the positive surface charge of the voids in the pure system, the average void in this aqueous solution is found to have a net negative charge. This is due to contributions from the water oxygen atoms that are negatively polarized by their intramolecular bonding.

Introduction

Aqueous solutions of tetrahydrofuran (THF) are a widely used solvent medium within the laboratory environment and have drawn considerable interest in regard to both their microscopic and mesoscopic physicochemical properties.[1−6] Despite their wide-ranging utility, the detailed understanding of their atomic-scale structure has been largely restricted to simulation studies,[1−3,5] although a few experimental investigations have recently become available that have used X-ray scattering,[4] nuclear magnetic resonance spectroscopy,[4] infrared spectroscopy,[6] and small-angle neutron scattering.[7] These studies have raised a number interesting issues in regard to the balance between the hydrogen-bonding interactions within the solvent water and the nonpolar interactions that occur between the nonpolar groups on the cyclic ether molecules themselves and also between these groups and the solute's hydration shell. The mixture of nonpolar and polar interactions in these solutions is thought to underlie the novel phase diagram for this system in which a closed loop of liquid−liquid immiscibility is seen to form in the intermediate concentration range and as the temperature of the mixture is raised into the 60−140 °C range.[8]

In this study, we present detailed experimental structural data on these important solvent solutions obtained using neutron diffraction with hydrogen/deuterium isotopic substitution directly coupled with modern atomistic computer modeling methods. These recently developed techniques allow us to extract, in unprecedented detail, both the spatially averaged structural correlations between the various atomic sites on the molecules and three-dimensional snapshots of the preferred orientational molecular configurations and extended liquid structure. A solution concentration of 0.23 mole fraction tetrahydrofuran was selected for this initial study because this corresponds to a concentration close to the center of the closed loop of liquid−liquid immiscibility. The resulting structural model thus forms a reasonable baseline for future studies of the phase separation phenomenon in this system where the concentrations of the water-rich and ether-rich immiscible phases are ∼0.09 and ∼0.39 mole fraction tetrahydrofuran, respectively.

Theory

Following data reduction, the function extracted from a neutron diffraction measurement is the interference differential cross section, or total structure factor $F(Q)$ (see, for example, Keen[9])

$$F(Q) = \sum_{\alpha \le \beta} (2 - \delta_{\alpha\beta}) c_\alpha c_\beta b_\alpha b_\beta [S_{\alpha\beta}(Q) - 1] \qquad (1)$$

Q is the magnitude of the momentum transfer vector in the scattering process for neutrons of wavelength λ, through a scattering angle 2θ, and is defined as

$$Q = \frac{4\pi}{\lambda} \sin\theta \qquad (2)$$

c_α, c_β and b_α, b_β are, respectively, the atomic fractions and neutron scattering lengths of each atom type in the sample that weight the sum of partial structure factors, $S_{\alpha\beta}(Q)$. These latter functions contain the structural information relating to the pairwise interactions between atoms of type α and β. $\delta_{\alpha\beta}$ is the Kronecker delta function used to avoid double counting the interactions between atoms of the same type.

Even though the $S_{\alpha\beta}(Q)$ terms contain all of the structural information relating to pair interactions between atoms, it is often more useful to consider the site−site pair distribution

* To whom correspondence should be addressed. E-mail: D.T.Bowron@rl.ac.uk.
† CCLRC Rutherford Appleton Laboratory.
‡ University College London.

10.1021/jp064170v CCC: $33.50
Published on Web 09/19/2006

functions, $g_{\alpha\beta}(r)$, obtained by Fourier transformation of the respective $S_{\alpha\beta}(Q)$ factors, i.e.

$$g_{\alpha\beta}(r) - 1 = \frac{1}{(2\pi)^3\rho}\int_0^\infty 4\pi Q^2[S_{\alpha\beta}(Q) - 1]\frac{\sin(Qr)}{Qr}\,\mathrm{d}Q \quad (3)$$

where ρ is the atomic density of the system and r is the distance between atoms. The positions of features within these functions directly correlate with interatomic distances in the sample, and if appropriately integrated, the areas beneath regions in $g_{\alpha\beta}(r)$ provide information about the number of neighboring atoms of type β around α and vice versa in the distance range selected; that is

$$N^{\beta}(\alpha) = \int_{r_1}^{r_2} 4\pi r^2 c_\beta \rho g_{\alpha\beta}(r)\,\mathrm{d}r \quad (4)$$

As a single neutron diffraction experiment allows the measurement of only the total structure factor for a system, it remains a challenge to determine the partial structure factors and site−site pair distribution functions that are required to fully characterize a multicomponent system. Techniques of neutron diffraction with isotopic substitution have gone some way toward solving this problem[10] and, in combination with modern computational methods,[11] now allow comprehensive three-dimensional structural models to be produced that are consistent with the experimental data. These, in turn, allow reasonable estimates of the partial structure functions to be obtained.

Experiment

Selective hydrogen/deuterium isotopic substitution was used to access the structural information relating to intermolecular correlations between the cyclic ether and water components of the investigated binary mixture. As the atomic sites on the tetrahydrofuran molecule that are available for H/D substitution do not undergo in-solution isotopic exchange, unlike those on the water molecule, it is possible to use a combination of seven experiments to cleanly access correlation function information that directly relates to the intermolecular interactions between the two mixture components, i.e., solute−solute, solvent−solvent, and solute−solvent terms.[10] The seven isotopically distinct samples measured, all at a concentration of 0.23 mole fraction tetrahydrofuran, were as follows: (1) $(CH_2)_4O$ in D_2O, (2) 1:1 mixture of $(CH_2)_4O$ and $(CD_2)_4O$ in D_2O, (3) $(CD_2)_4O$ in D_2O, (4) $(CD_2)_4O$ in a 1:1 mixture of H_2O and D_2O, (5) $(CD_2)_4O$ in H_2O, (6) 1:1 mixture of $(CH_2)_4O$ and $(CD_2)_4O$ in a 1:1 mixture of H_2O and D_2O, and (7) $(CH_2)_4O$ in H_2O.

First, using second-order difference techniques,[12] samples 1−3 weight the structural information toward the solute−solute interactions between tetrahydrofuran molecules, from the viewpoint of the correlations between the hydrogen/deuterium sites around the cyclic ether ring. Next, samples 3−5 provide structural information weighted toward the solvent−solvent correlations between water molecules from the viewpoint of the solvent's hydrogen/deuterium sites. Finally, samples 3, 6, and 7, in combination with the results from samples 1−5 provide information weighted toward the structural cross-correlations between the solute THF molecules and the solvent water molecules.

The use of isotopic substitution methods on the tetrahydrofuran−water system for the study of structural properties places certain restrictions on the thermodynamic conditions under which the system can be studied. Recent experimental investigations of the system's phase diagram have shown that isotopic variation has a significant impact on the miscibility of the two components.[13,14] Changes in the degree of deuteration affect both the concentration and temperature dependence of the mixture's well-known closed-loop region of liquid−liquid immiscibility.[8] The lower and upper critical solution points have been found to be particularly sensitive to small changes in the strength of the hydrogen bonding in the solvent water and between the solute and solvent that are induced by deuteration.[14] Phase separation would prevent difference-based structural studies of the type discussed here, as the separated components would have distinct concentrations and structures that would differ between isotopic analogues. To avoid these difficulties, this study was undertaken at room temperature where the isotopic solutions are all deemed to be well mixed with only short-range concentration fluctuations in evidence.[15] The solutions are thus considered sufficiently far from any critical point to avoid amplification of structural differences that would depend on the slight hydrogen-bond strength variations to a level where they would impact the underlying assumptions of the technique.

The diffraction measurements were performed at the ISIS spallation neutron source at the Rutherford Appleton Laboratory, Chilton, Didcot, Oxon, U.K., using the Small Angle Diffractometer for Amorphous and Liquid Samples (SANDALS). This instrument is optimized for the study of light-element-containing samples through its use of high-energy neutrons and its configuration of low-angle detector banks covering the range from 3° to 40° in 2θ, the scattering angle. The measurements were made at the ambient temperature of the instrument (20 °C), and the samples were contained in flat cells of internal dimensions 1 mm × 35 mm × 35 mm, bounded by null-scattering $Ti_{0.68}Zr_{0.32}$ alloy walls of 1.1-mm thickness. The data were analyzed in the wavelength range from 0.05 to 3.5 Å using the Gudrun package[16] that is based on the algorithms outlined in the widely used Atlas package.[17] These routines correct the data for background, absorption, and multiple scattering and normalize the results to an absolute scale using the scattering measured for a vanadium standard. The final corrections for self-scattering and inelastic scattering were performed using the methods outlined in Soper and Luzar.[18]

Data Modeling

To maximize the information that can be extracted from the seven neutron scattering measurements, an ensemble of three-dimensional structural models of the liquid mixture was created using the technique of empirical potential structure refinement (EPSR).[19,20] In this method, a Monte Carlo simulation of the liquid structure is generated, initially using standard classical potentials based on Lennard-Jones parameters and charges. Once equilibrated, the simulation is compared with the available experimental data, and a perturbation potential is derived. This perturbation potential is based on the difference between the scattering patterns calculated from the current model and the experimental data. The simulation then proceeds allowing the perturbation potential to evolve under an iterative mechanism until such a point where the atomic and molecular configurations calculated from the model are considered an acceptable match to the experimental data. Once the perturbation potential has been refined, the Monte Carlo modeling is continued under the sum of the reference plus perturbation potentials, and structural information is extracted via ensemble averages. In such a way, it is thus possible to refine a single three-dimensional model for the liquid that is simultaneously consistent with all seven isotopically distinct data sets while also maintaining fundamental constraints such as the known structure of the molecules within the mixture and the appropriate atomic density for the liquid.

TABLE 1: Lennard-Jones, Charge, and Atomic Mass Parameters Used for the Reference Potentials that Seed the Empirical Potential Structure Refinement Model for 0.23 Mole Fraction Tetrahydrofuran in Water

atom type	ϵ (kJ mol^{-1})	σ (Å)	M (amu)	q (e)
O	0.586	2.90	16	−0.400
C1	1.251	3.21	12	0.140
C2	1.251	3.21	12	0.000
M1	0.791	2.58	2	0.030
M2	0.791	2.58	2	0.000
OW	0.650	3.17	16	−0.8476
HW	0.000	0.00	2	0.4238

In this study, the following labels were assigned to the atomic sites on the tetrahydrofuran molecule: O for the ether oxygen within the five-membered ring; C1 for the carbon atoms that are connected to the oxygen atom; C2 for the carbon atoms connected only to other carbon atoms; and M1 and M2 for the hydrogen atoms bonded to carbon atoms C1 and C2, respectively. The atomic sites on the water molecules were assigned the labels of OW and HW for the water oxygen atom, and the two hydrogen atoms, respectively. The Lennard-Jones parameters, atomic masses and fractional charges used to seed the modeling process are summarized in Table 1.

The simulation was initialized in a cubic box of side length 34.87 Å containing 184 tetrahydrofuran molecules and 616 water molecules corresponding to an atomic density of 0.1 atom Å^{-3}. To enable comparison of the diffraction data calculated from the model, the configuration of individual molecular units within the simulation was periodically varied within harmonic constraints while maintaining the general structure of each molecule.[21] This process is a necessary addition to the standard Monte Carlo simulation method, as the real experimental data reflect Debye−Waller broadening of the real-space correlations caused by zero-point-energy effects.

Results

Figure 1 shows the experimental structure factor data collected for the seven isotopically distinct samples of tetrahydrofuran in water, along with the fit and fit residual produced by the EPSR modeling. Overall, the quality of the fit is good, although some deviation at low Q is seen in the fit residuals. In general, these residuals are found to correspond to low-frequency components that would contribute to real-space features at unphysically short interatomic distances. Such residuals generally result from background components that remain following the final data corrections for inelastic scattering processes, and it is a particular strength of the EPSR analysis method that the models are built to avoid bias from such unphysical data features that would plague more traditional data interpretation schemes.

The data from protonated tetrahydrofuran in deuterated water (C_4H_8O in D_2O) and deuterated tetrahydrofuran in protonated water (C_4D_8O in H_2O) display a degree of small-angle scattering. This reflects the presence of the small concentration fluctuations or aggregation/segregation phenomena between the two components in the binary mixture[4,7] that are known to increase with temperature as one approaches the lower critical solution temperature.[7,15] For these particular isotopic compositions, the visibility of these fluctuations is enhanced by the contrast in scattering lengths between the hydrogen and deuterium sites that differ between the solute and solvent molecules. The ability of the EPSR model to reproduce the data in the low-Q region for these isotopic compositions confirms that the size of the cubic model box, at 34.9 Å per side, is sufficient to allow for this phenomenon in regard to structural investigations on intermolecular length scales.

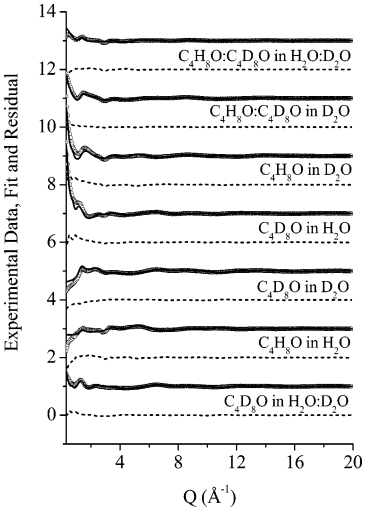

Figure 1. Experimentally measured total structure factor data (open circles) and EPSR refined fits (solid lines) for neutron scattering data collected on the isotopically distinct 0.23 mole fraction solutions of tetrahydrofuran in water. The fit residuals (broken lines) are shown offset for clarity.

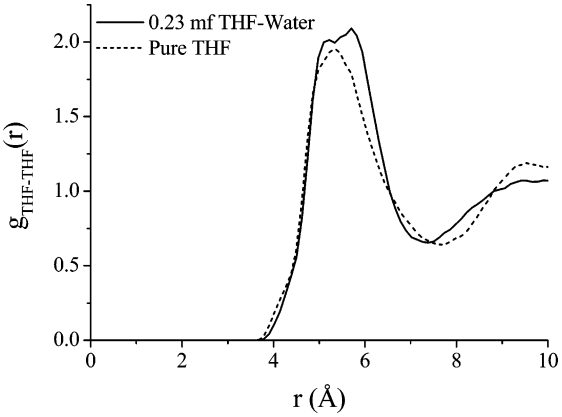

Figure 2. EPSR-derived molecular-centers distribution function between tetrahydrofuran molecules in 0.23 mole fraction aqueous solution (solid line) at room temperature. The center of the molecule is defined as the geometric center of the oxygen atom and four carbon atoms that make up the five-membered ring. For comparison, the corresponding molecular-centers function obtained from the pure liquid (broken line) is also shown.

Figure 2 shows the pair distribution function of geometric ring centers characterizing the orientationally averaged correlations between tetrahydrofuran molecules in the 0.23 mole fraction aqueous solution compared to the corresponding function obtained for the pure liquid.[22] It is evident that the presence of the solvent water acts to shift the average center distance between tetrahydrofuran molecules to greater values (from ∼5.3 to ∼5.5 Å) while tightening the interactions, as evidenced by the shift to lower distances of the first minimum (from ∼7.6 to ∼7.3 Å). The corresponding coordination numbers for the distance range between 3.6 and 7.6 Å are 12.6 ± 0.3 for the pure liquid and 7.9 ± 0.3 for the 0.23 mole fraction solution. This indicates that, in the 0.23 mole fraction aqueous solution, four of the tetrahydrofuran molecules that would make up one-third of the first coordination shell in the pure liquid have been replaced by water molecules, as will be illustrated below.

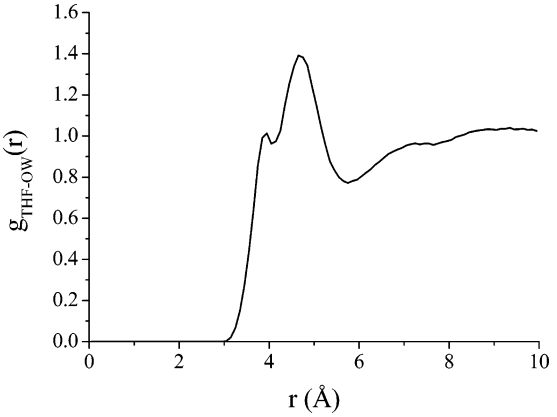

Figure 3. EPSR-derived molecular-centers distribution function between tetrahydrofuran and water in 0.23 mole fraction aqueous solution (solid line) at room temperature. The center of the THF molecule is defined as the geometric center of the oxygen atom and four carbon atoms that make up the five-membered ring, and the assigned center of the water molecule is the position of the molecule's oxygen atom.

Figure 3 allows for the evaluation of the distribution of these water molecules as a function of the correlations between the geometric ring center and the oxygen atoms of the hydrating water molecules. The hydration shell of THF is indicated by a double-peaked structure in the distance range between 3.0 and 5.75 Å. The first peak at 3.95 Å corresponds approximately to the two water molecules that might be expected to be able to hydrogen bond to the ether oxygen site. The second peak in the pair distribution function of the THF−OW centers, at 4.7 Å, corresponds to an additional eight water molecules that hydrate the nonpolar regions of the solute molecule. The coordination numbers and distance ranges to which they correspond are reported in Table 2, along with a selection of characteristic coordination numbers determined for other correlations in the system.

Figures 4−6 show the remaining site−site pair distribution functions relating to the atomic site−site intermolecular correlations between tetrahydrofuran molecules and between tetrahydrofuran and water molecules. In particular, a significant function of interest is the $g_{O-HW}(r)$ site−site distribution function that shows the nature of the hydrogen-bonding interactions between the hydrogen-bond-acceptor site on the ether molecule and the hydrogen sites donated from solvating water molecules. The coordination numbers corresponding to the interaction between these sites are included in Table 2 and indicate that approximately one water hydrogen atom is, on average, strongly associated with the ether oxygen site at a distance of 1.77 Å, with two additional hydrogen atoms associated with water molecules in the distance range from 2.46 to 3.6 Å. Naturally, one of these additional hydrogen atoms will be associated with the water molecule contributing the short-range hydrogen-bonded interaction at 1.77 Å, whereas the second must come from an additional water molecule that, on average, will be found in this extended distance range. The finding that, on average, only one water molecule is directly bonded to the ether oxygen is somewhat surprising but can be understood in the context of the other site−site distribution functions. Table 2 and $g_{O-M1}(r)$ indicate that, on average, there is a short-range interaction between ether oxygens and one of the slightly positively polarized M1 hydrogens on a neighboring tetrahydrofuran molecule. Such an interaction in the 2.3−3.5-Å range would sterically hinder the possibility of placing two water molecules in a direct hydrogen-bonded configuration with a single oxygen site and accounts for why the extra water hydrogen is found in the 2.46−3.6-Å range.

TABLE 2: Coordination Numbers Obtained by Integration of the Features in the Indicated Site−Site Distribution Functions

correlation	R_{min} (Å)	R_{max} (Å)	atomic density (atom Å^{-3})	coordination no. (atoms)
THF−THF	3.6	7.0	0.00434	6.7 ±0.3
	3.6	7.6		7.9 ± 0.3
O−O	2.6	5.3	0.00434	2.0 ± 0.1
	5.3	8.7		9.9 ± 0.3
O−M1	2.3	3.5	0.01736	1.2 ± 0.1
M1−O	2.3	3.5		0.3 ± 0.02
THF−OW	3.0	4.15	0.01453	1.7 ± 0.1
	4.15	5.75		8.1 ± 0.2
	3.0	5.75		9.7 ± 0.2
OW−THF	3.0	4.15	0.00434	0.5 ± 0.1
	4.15	5.75		2.4 ± 0.1
	3.0	5.75		2.8 ± 0.1
O−OW	2.3	3.4	0.01453	1.2 ± 0.1
	3.4	4.4		2.0 ± 0.1
	4.4	5.2		3.3 ± 0.1
	5.2	6.7		9.10 ± 0.1
OW−O	2.3	3.4	0.00434	0.3 ± 0.02
	3.4	4.4		0.6 ± 0.03
	4.4	5.2		1.0 ± 0.04
	5.2	6.7		2.7 ± 0.1
O−HW	1.2	2.46	0.02906	0.9 ± 0.1
	2.46	3.6		2.2 ± 0.1
HW−O	1.2	2.46	0.00434	0.13 ± 0.01
	2.46	3.6		0.33 ± 0.02
M1−OW	2.3	3.7	0.01453	1.7 ± 0.05
OW−M1	2.3	3.7	0.01736	2.0 ± 0.1
OW−OW	2.4	3.3	0.01453	3.2 ± 0.1
	3.3	4.6		4.9 ± 0.1
	2.4	4.6		8.0 ± 0.2
OW−HW	1.2	2.3	0.02906	1.3 ± 0.1
HW−OW	1.2	2.3	0.01453	0.7 ± 0.02
HW−HW	1.0	2.73	0.02906	2.8 ± 0.1
	2.73	4.86		15.9 ± 0.2

Figure 7 shows the partial pair distribution functions that relate to the structure of the solvent water in the presence of the solute. In this aqueous solution, the function $g_{OW-OW}(r)$ is found to be markedly different from that of pure liquid water,[23] and the shoulder on the right-hand side of the first peak bears striking similarities to the OW−OW partial distribution function estimated for the compressed/high-density form of liquid water[24] or the solid very high-density amorphous ice (VHDA).[25] Although the form of this distribution function is similar to those of these high-density phases, the coordination numbers reported in Table 2 reveal that the structural details are significantly different. Integration of the first peak in $g_{OW-OW}(r)$ between 2.4 and 3.3 Å indicates that each water oxygen in the solution has 3.2 ± 0.1 neighbors in this range, whereas the corresponding integration for the first peak in VHDA gives an average coordination number of 4.1 ± 0.1 in the distance range between 2.3 and 3.1 Å. The shoulder to the right of the first peak in the tetrahydrofuran−water mixture has a coordination number of 4.9±0.1 water oxygen atoms, whereas in pure VHDA, this feature integrates to eight neighboring water molecules in the corresponding distance range of 3.1−4.1 Å. Thus, although the $g_{OW-OW}(r)$ functions are superficially similar, the local structures of these systems are clearly different.

An additional important feature to note in $g_{OW-OW}(r)$ that can also be seen in $g_{OW-HW}(r)$ and $g_{HW-HW}(r)$ is the marked rise at low r. This indicates that an excluded-volume effect occurs in the THF−water mixture that has a tendency to spatially confine the water molecules and partially segregate them within the solution. This supports the conclusion that,

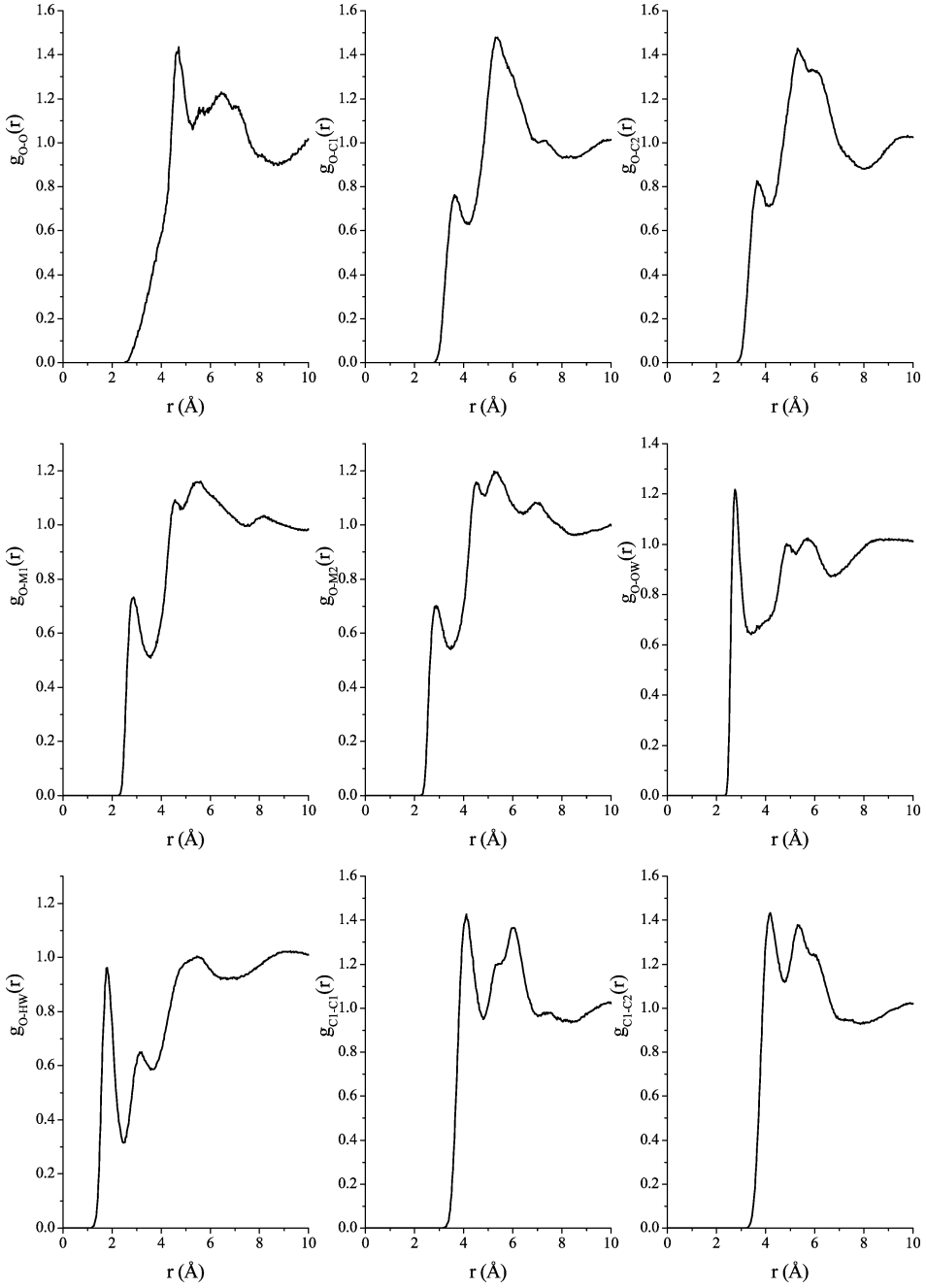

Figure 4. Intermolecular partial distribution functions derived by EPSR procedure 1, i.e., O−O, O−C1, O−C2, O−M1, O−M2, O−OW, O−HW, C1−C1, C1−C2, for 0.23 mole fraction tetrahydrofuran in water at room temperature.

even at room temperature, well below the region of liquid−liquid immiscibility, there is already a tendency in these solutions to try to separate the molecular components on the molecular length scales, though under the conditions of the experiment (20°C and ambient pressure), the system is still macroscopically well mixed.

The sum of the coordination number of the first peak in $g_{OW-OW}(r)$, 3.2 ± 0.1, with the coordination number of the first peak in $g_{OW-O}(r)$ [$=g_{O-OW}(r)$], 0.3 ± 0.02, accounts for all potential hydrogen bonding to oxygen sites that a water molecule can experience in this system. We find that this value is smaller than that of liquid water,[26] ∼4.3, and this, in turn, suggests that the presence of the solute tetrahydrofuran molecules disrupts the degree of general four-fold tetrahedral coordination in the solvent water network, in contrast to the findings in either the pure high-density water or amorphous ice system. This disruption to the first-shell ordering of the solvent water is also evident in the integral of the first peak in $g_{OW-HW}(r)$, which corresponds to the intermolecular hydrogen bonding between water molecules. In pure liquid water and the known ice phases, this peak integrates to each water oxygen atom having two hydrogen-bonded neighbors, whereas in this 0.23 mole fraction solution, each water molecule has on average 1.3 ± 0.1 accepted hydrogen-bonded neighbors (Table 2), which must reflect the ability of the solute tetrahydrofuran molecules to compete in this type of interaction by their ability to accept hydrogen bonds from, but not donate hydrogen bonds to, the solvent.

Three-Dimensional Solution Structure

To better visualize the three-dimensional structure of the binary solution, the spatial density functions $g_c(r,\Omega)$ were

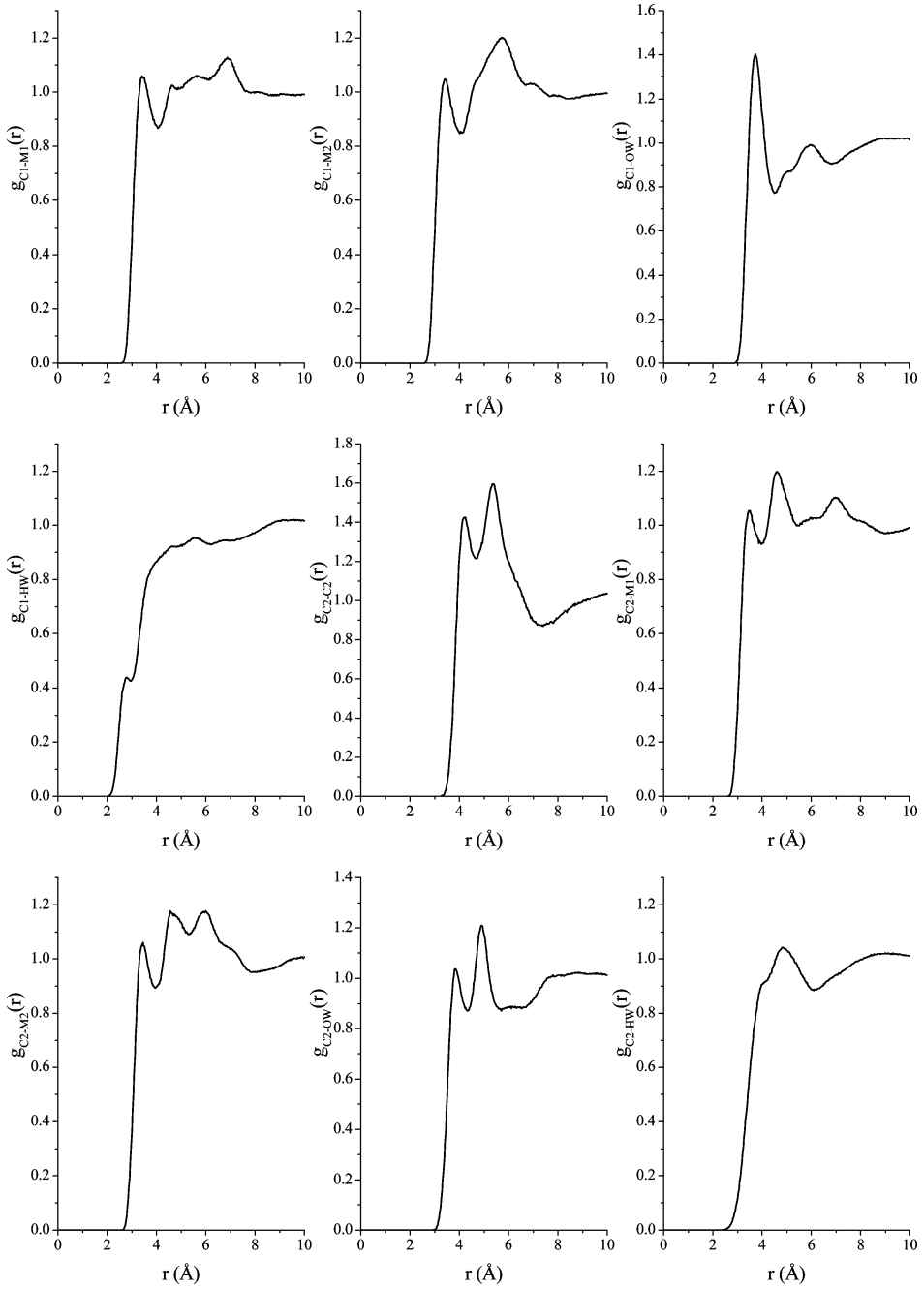

Figure 5. Intermolecular partial distribution functions derived by EPSR procedure 2, i.e., C1−M1, C1−M2, C1−OW, C1−HW, C2−C2, C2−M1, C2−M2, C2−OW, C2−HW, for 0.23 mole fraction tetrahydrofuran in water at room temperature.

calculated.[27] These quantities represent a three-dimensional map of the density of molecular centers of one molecular species about another, as a function of radial distance r and orientation $\Omega = (\theta, \phi)$, relative to the molecule placed at the origin but averaged over all angular orientations of the neighboring molecule. Figure 8 shows the coordinate reference frame utilized for the spatial density study.

Figure 9 shows the like-molecular-species spatial density functions corresponding to interactions between tetrahydrofuran molecules and between water molecules. First, considering Figure 9A, we note a distribution of tetrahydrofuran molecules around the central molecule that generally reflects a range of nonpolar and polar interactions similar to those found for the intermolecular correlations in the pure tetrahydrofuran system,[22] shown in Figure 9B for comparison. In the case of the aqueous solution, the relative spatial extent and balance of the bands and lobes of intensity can be seen to be somewhat different. The nonpolar interactions between tetrahydrofuran molecules are still found in the three bands of intensity above the central molecule and to either side of the molecule, centered on the plane of the central ring, but the more polar interactions between the cyclic ether molecules in the aqueous solution are now more spatially localized. This can be seen in the distinct lobes of intensity out of the ring plane and mediated by the oxygen atom of the central molecule. Of particular note in the aqueous system is the suppression of the intensity in the tetrahydrofuran−tetrahydrofuran spatial density function immediately below the polar oxygen site in the ring of the central molecule. Recalling from the earlier discussion of the coordination numbers for tetrahydrofuran molecules around other tetrahydrofuran molecules, the addition of water to the system appears to have had the effect of enhancing the localization of the polar interactions

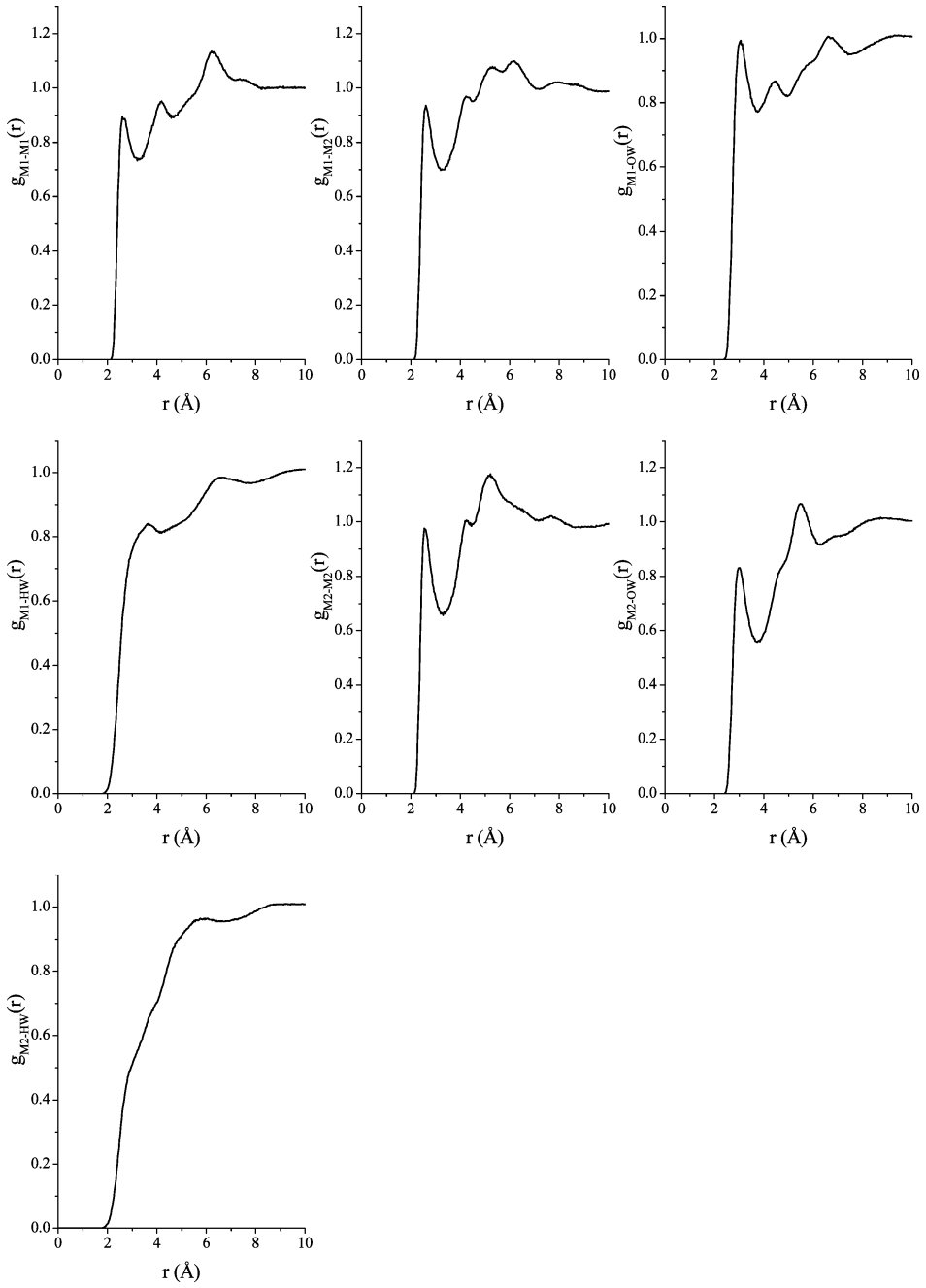

Figure 6. Intermolecular partial distribution functions derived by EPSR procedure 3, i.e., M1−M1, M1−M2, M1−OW, M1−HW, M2−M2, M2−OW, M2−HW, for 0.23 mole fraction tetrahydrofuran in water at room temperature.

between the ether molecules and reducing their overall extent. This reflects the reduction of the average 12.6 molecular neighbors in the pure ether to approximately 8 tetrahydrofuran neighbors in the aqueous system.

Figure 9C shows the most preferable distribution of water oxygen atoms around an arbitrarily selected central water molecule and highlights the disruptive effect that the solute tetrahydrofuran induces on the water−water hydrogen-bonding configurations compared to the pure liquid reference.[28] Even though the preferred hydrogen-bonding interactions mediated by the hydrogen donor sites on the central molecule seem to be very similar in orientation to those in the pure liquid, the position of the lobes most closely associated with the oxygen atom of the central water molecule, the hydrogen-bond-acceptor site, are more orientationally defined. These lobes in the lower half of the figure highlight both the traditional positions of neighboring water molecules in the positive and negative directions along the *x* axis, and also now, slightly more distant and in the positive and negative directions of the *y* axis, there appear two additional regions of preferred occupation. Recalling the discussion regarding the functional form of the $g_{OW-OW}(r)$ partial distribution function and its striking similarity to those observed for the high-density forms of liquid water and amorphous ice, we can now better judge and compare the structure in the solvent environment. We see from the spatial density function that, despite the similarities in the pair distribution functions, the spatial distribution of the compressed water structure is quite different.[25] In the very high-density ice phase, the compression of the water structure results in neighboring water molecules occupying sites in nonbonding positions between the central water molecule's hydrogen-bond-donor sites. In marked contrast, the compressed water structure in 0.23 mole fraction tetrahy-

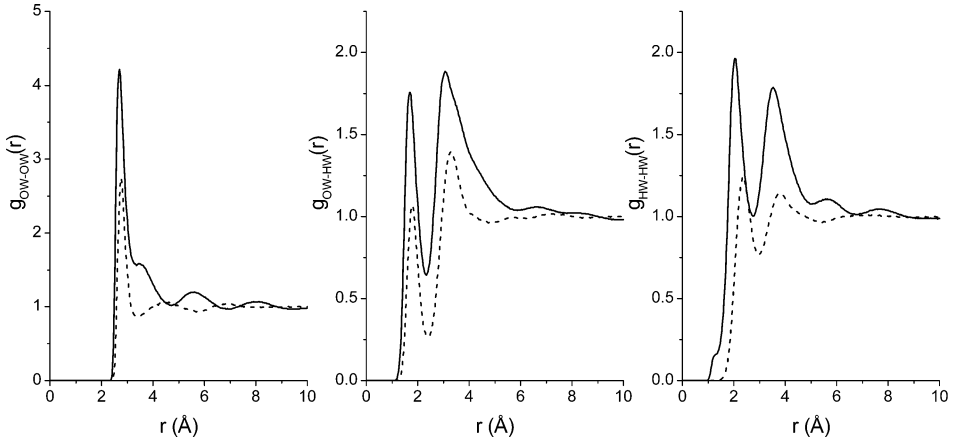

Figure 7. Intermolecular partial distribution functions for the water structure in 0.23 mole fraction tetrahydrofuran in water at room temperature derived by the EPSR procedure: OW−OW, OW−HW, HW−HW (solid lines). The corresponding functions for the pure-water partial distribution functions are included for comparison (broken lines). The pure-water functions were generated using the same EPSR procedure applied to neutron scattering data on H_2O, D_2O, and HDO obtained at 25 °C.

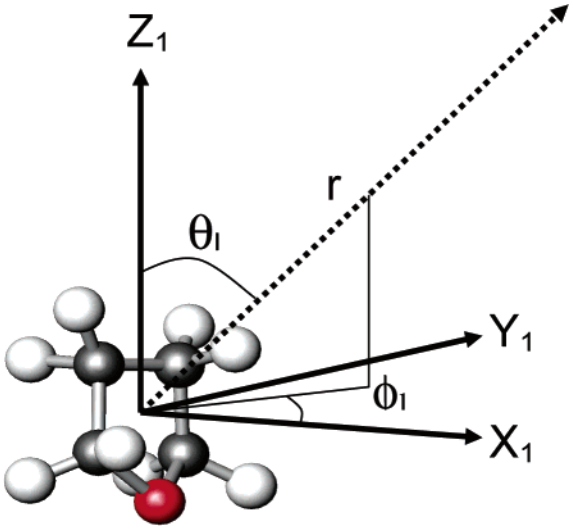

Figure 8. Coordinate axis reference frames of the tetrahydrofuran molecule used to calculate the spatial density functions of surrounding molecules.

drofuran solution arises from the development of first-neighbor coordination sites on either side of the usual hydrogen-bond-acceptor sites of the central molecule, giving rise to an octahedral-like local coordination, as opposed to the more normal tetrahedral coordination in pure water.

Turning our attention to the molecular cross-correlations, Figure 10 shows the spatial density functions for the interactions between tetrahydrofuran and water and vice versa. Figure 10A shows the preferred location of the two water molecules that contribute to the first peak in Figure 3. This feature was previously assigned to water molecules positioned advantageously for hydrogen-bonding interactions with the oxygen atom in the ether ring and is confirmed by this spatial density function. Figure 10B shows the preferred position for water molecules in a slightly larger distance range and highlights the nonpolar (hydrophobic) hydration shell of the tetrahydrofuran molecule and the extended polar interaction region corresponding to the H-bond-accepting ring oxygen site. Panels C and D of Figure 10 show the corresponding spatial density functions placing the water molecule at the origin and plotting the preferred location of the geometric centers of the neighboring tetrahydrofuran molecules.

Figure 10C displays similarities with the distribution of water molecules about water in the pure solvent, albeit at a greater distance because of the larger size of the tetrahydrofuran molecules. This distribution is interesting considering the fact that the tetrahydrofuran molecule can only accept hydrogen bonds. The two lobes above the water hydrogen sites along the positive and negative *y* axis correspond to the relative position of the tetrahydrofuran ring center when the water molecule is coordinated to the H-bond-accepting oxygen site on the cyclic ether. If we now take into consideration the positions and coordination numbers of the first peaks in the $g_{O-OW}(r)$ and $g_{O-HW}(r)$ partial distribution functions at 2.71 and 1.77 Å respectively, as well as the peak in $g_{O-O}(r)$ found at 4.66 Å, it appears that a common structural motif within the liquid mixture is a water-bridged interaction between the polar oxygen sites of two neighboring tetrahydrofuran molecules. The remaining band of intensity in this spatial density function, below the central water molecule oxygen atom, in contrast, reflects the angular distribution of the tetrahydrofuran ring center available when the water oxygen atom coordinates the slightly positively polarized ring hydrogens (M1) bound to the carbon atoms that are bonded to the ether oxygen.

Figure 10D shows the form of the distribution of tetrahydrofuran centers about a central water molecule in the distance region corresponding to the hydrophobic hydration shell shown in Figure 10B. Loosely speaking, the intensity in the upper half of the figure, corresponding to regions parallel to the plane of the central water molecule and between the two water hydrogen atoms, corresponds to tangential orientations of the water molecules relative to the surface of the hydrophobic hydration shell. The intensity in the lower half of the figure, around the water oxygen site, corresponds to the more distant interactions that occur between the water molecule and the polarized regions of neighboring tetrahydrofuran molecules. The shape of this second shell again loosely resembles that of the second shell of pure water, albeit at a greater distance from the central molecule.[26]

Void Structure

A key characteristic of pure liquid tetrahydrofuran is an intrinsic degree of void space within the molecular network that arises from the awkward packing of the molecular units.[22,29] In the pure system, these void spaces are found to have a slight positive charge polarization on the bounding surfaces, due to

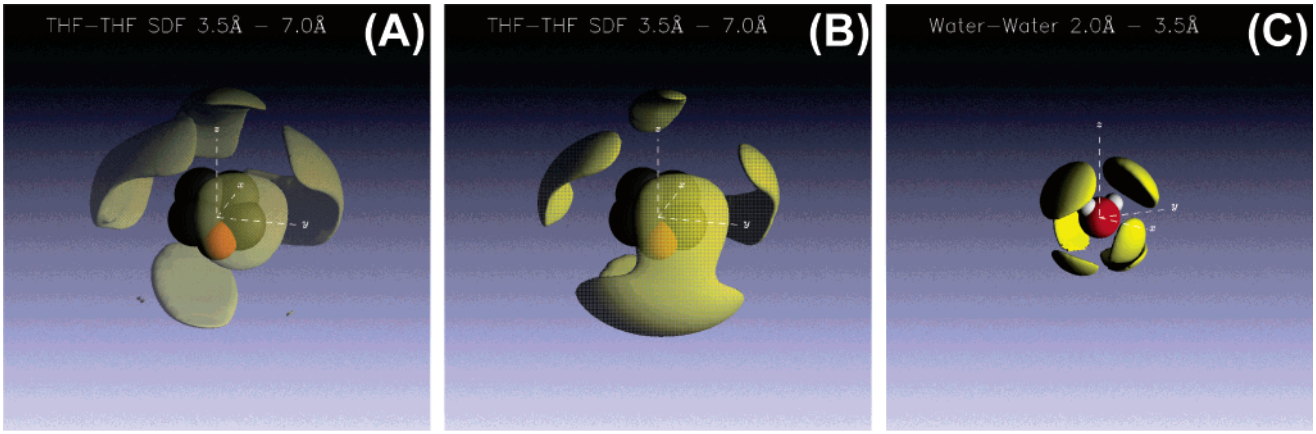

Figure 9. EPSR-derived spatial density functions: (A) $g_{THF-THF}(r,\Omega)$ in the 0.23 mole fraction tetrahydrofuran−water system, (B) $g_{THF-THF}(r,\Omega)$ in pure ether[21] for comparison, and (C) $g_{water-water}(r,\Omega)$ in the aqueous solution. These results show (A,B,) the distribution of tetrahydrofuran molecular centers around a central tetrahydrofuran molecule and (C) the distribution of water molecules around a central water molecule as functions of the distance r and orientation $\Omega = (\theta, \phi)$. For the THF−THF spatial density function, the isosurface is calculated to show the most probable regions of space that would be occupied by the top 30% of the neighboring molecules that make up the complete coordination shell in the distance range from 3.5 to 7 Å. For the water−water spatial density function, the isosurface is set to the most probable 40% of neighboring molecules in the distance range from 2.0 to 3.5 Å. The scale of the viewport window in all three panels is ±10 Å.

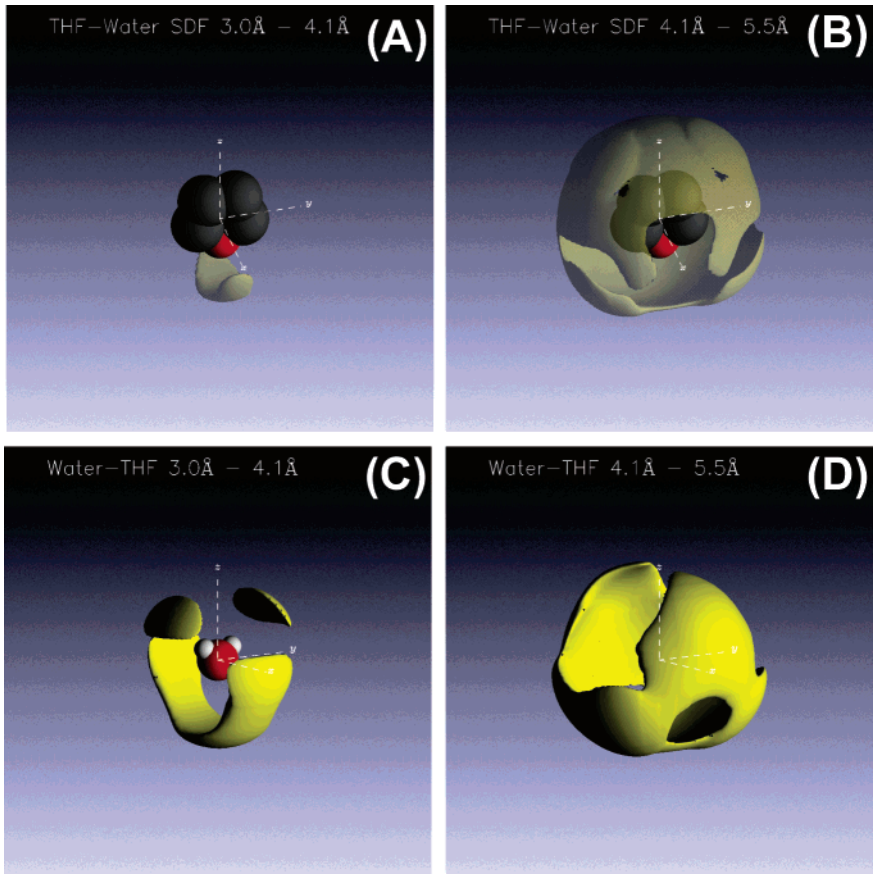

Figure 10. EPSR-derived spatial density functions: (A) $g_{THF-water}(r,\Omega)$ in the distance range from 3.0 to 4.1 Å at an isosurface level corresponding to the top 50% of molecules that make up the coordination shell, (B) $g_{THF-water}(r,\Omega)$ in the distance range from 4.1 to 5.5 Å at an isosurface level corresponding to the top 40% of molecules within the shell, (C) $g_{water-THF}(r,\Omega)$ in the distance range from 3.0 to 4.1 Å at an isosurface level of 90%, and (D) $g_{water-THF}(r,\Omega)$ in the distance range from 4.1 to 5.5 Å at an isosurface level of 40%. These results show (A,B) the distribution of water molecular centers around a central tetrahydrofuran molecule and (C,D) the distribution of tetrahydrofuran molecule centers around a central water molecule as functions of the distance r and orientation $\Omega = (\theta, \phi)$. The scale of the viewport window in all panels is ±10 Å.

the dominance of M1 and M2 atoms in these positions. Although their shape is not regular, the typical size of the voids in the pure system corresponds to a radius of 1.25 Å defined using the surface of the bounding atoms. It is thus interesting to consider the impact that the addition of approximately three water molecules for every tetrahydrofuran molecule would have on this characteristic feature.

Figure 11 shows a typical distribution of void-like regions found using the same radius criterion of 1.25 Å and the Lennard-Jones parameters of Table 1 to estimate the atomic radii. To

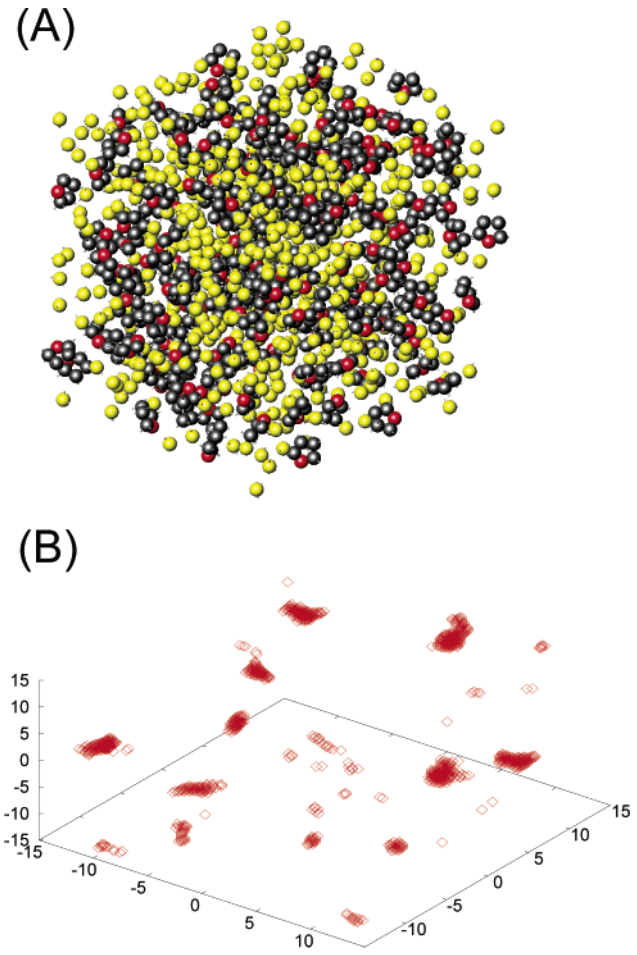

Figure 11. (A) Snapshot of the EPSR refined three-dimensional structure of 0.23 mole fraction tetrahydrofuran in water, color highlighted to show the THF carbon and oxygen atoms in black and red and the water oxygen atoms in yellow. This allows one to visualize the microscopic segregation of the two mixture components highlighted in the discussion. (B) Void regions within a typical model box where the nearest atomic surface is farther than 1.25 Å from a highlighted point.

perform the calculation, it was necessary to assign a Lennard-Jones σ value (here, 2.0 Å) to the water hydrogen atoms, as the SPC/E parameters used to seed the water molecules do not assign a specific radius to the site. Despite the fact that the water molecules are small and can thus more effectively fill the spaces resulting from the awkward packing of the tetrahydrofuran molecules, the quantity and distribution of the void spaces in the mixture is found to be very similar to that in the pure cyclic ether.

Figure 12 presents the average void surface interaction percentages for the various atom types within the mixture. This histogram shows the surface chemistry based on finding the nearest atom type to each point determined to be within a void region. It is immediately evident that the surface chemistry of the void spaces in the aqueous solution is no longer dominated by the M1 and M2 atom types found in pure tetrahydrofuran.[21] In the aqueous solution, approximately 40% of the closest surface interactions in the void space are now with the negatively polarized water oxygen sites, and 8% are with the positively polarized water hydrogen sites. The surface interactions with the hydrogen sites on the cyclic ether have been reduced to approximately 25% with the positively polarized M1 sites and 25% with the electrically neutral M2 sites, from levels of approximately 40% and 55%, respectively, for the M1 and M2

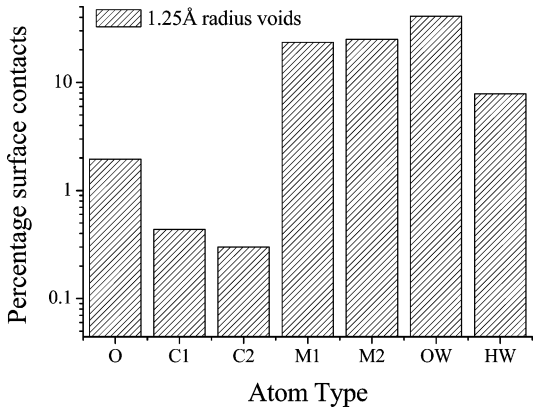

Figure 12. Void surface histogram showing the percentage of each atom type that bound the void-like regions within the liquid. Note the logarithmic ordinate scale.

sites in the pure ether.[22] Using the partial charges given in Table 1, the average electrostatic character of the surface of the voids in the aqueous solution is now seen to be significantly negatively charged, as opposed to the slight positive polarization of the void spaces found in the pure organic liquid.

Conclusions

This study highlights a rich range of novel structural characteristics in the widely used, but previously poorly characterized solvent medium of tetrahydrofuran in water. First, the results demonstrate a striking example of hydrophobic interactions where adding water molecules induces a relative increase in the degree of nonpolar interactions between the ether molecules by enhancing the spatial localization of the polar interactions and a reduction in the number of such interactions involving the oxygen sites between ether molecule rings. The presence of water molecules also facilitates water-mediated interactions between the ether oxygens. Second, the presence of the hydrogen-bond-accepting tetrahydrofuran molecule in the solvent water dramatically changes the nature of the water−water interactions themselves. In pure water, the number of hydrogen-bond-donor and -acceptor sites is balanced, but the addition of tetrahydrofuran leads to an excess of the latter. This imbalance results in an effective compressive effect upon the near-neighbor interactions between water molecules, although, in contrast to the reorganization that is induced by the direct application of pressure where neighboring water molecules take up occupation of nonbonding sites between hydrogen sites, the effect of this cyclic ether solute is to enhance interactions occurring around the lone-pair region of the water molecules.

The findings relating to void structure suggest the interesting possibility that, by choosing the level of water added to liquid tetrahydrofuran, it might be possible to control the *average* electrostatic character of the small void spaces that would be encountered within the liquid. This, in turn, might provide a new means to refine investigations into processes such as charge-transfer-to-solvent-type chemical reactions.[30] The void spaces within the mixture would be expected to be present at least to the solution concentration studied here of approximately three water molecules for each tetrahydrofuran molecule. The more water is added to the system, the less likely it would be to find regions in the liquid subject purely to tetrahydrofuran molecule interactions, and this can, in turn, be expected to affect the balance between the number of voids with positive electrostatic character and the number with negative character. It is important to remember that the voids themselves are dynamic entities that

will spontaneously form and disappear as the molecules move within the liquid medium. In a system, as studied here, where the negative polarization of the water oxygen atom is significantly greater than the positive polarization of the hydrogen sites on the cyclic ether, the presence of a single water oxygen in the surface of a void space would likely switch its net electrostatic character from positive to negative.

Acknowledgment. We thank the Engineering and Physical Sciences Research Council for funding under Grant GR/K/12465 and the Council for the Central Laboratory of the Research Councils for access to their neutron facility, ISIS, Rutherford Appleton Laboratory, Oxfordshire, U.K.

References and Notes

(1) Freitas, L. C. G.; Cordeiro, J. M. M. *J. Mol. Struct. (THEOCHEM)* **1995**, *335*, 189.
(2) Brovchenko, I.; Guillot, B. *Fluid Phase Equilib.* **2001**, *183*−*184*, 311.
(3) Oleinikova, A.; Brovchenko, I.; Geiger, A.; Guillot, B. *J. Chem. Phys.* **2002**, *117*, 3296.
(4) Takamuku, T.; Nakamizo, A.; Tabata, M.; Yoshida, K.; Yamaguchi, T.; Otomo, T. *J. Mol. Liq.* **2003**, *103*−*104*, 143.
(5) Brovchenko, I.; Geiger A.; Oleinikova, A. *Phys. Chem. Chem. Phys.* **2004**, *6*, 1982.
(6) Stangret J.; Gampe, T. *J. Mol. Struct.* **2005**, *734*, 183.
(7) Finney, J. L. *Faraday Discuss.* **1996**, *103*, 1.
(8) Matouš, J.; Hrncirik, J.; Novák J. P.; _Sobr, J. *Collect. Czech. Chem. Commun.* **1970**, *35*, 1904.
(9) Keen, D. A. *J. Appl. Crystallogr.* **2001**, *34*, 172.
(10) Finney J. L.; Soper, A. K. *Chem. Soc. Rev.* **1994**, *23*, 1.
(11) McGreevy, R. L. *J. Phys. Condens. Matter* **2001**, *13*, R877.
(12) Bowron, D. T.; Finney, J. L.; Soper, A. K. *J. Phys. Chem. B* **1998**, *102*, 3551.
(13) Balevicius, V.; Weiden, N.; Weiss, A. *Ber. Bunsen-Ges. Phys. Chem.* **1994**, *98*, 785.
(14) Oleinikova, A.; Weingärtner, H. *Chem. Phys. Lett.* **2000**, *319*, 119.
(15) Bowron, D. T.; Finney, J. L. Experimental Report 6-02-139; Institute Laue-Langevin: Grenoble, France, 1996.
(16) Soper, A. K. Rutherford Appleton Laboratory, Chilton, Didcot, Oxon, U.K. Private communication, 2005.
(17) Soper, A. K.; Howells, W. S.; Hannon, A. C.; *ATLAS*—*Analysis of Time-of-Flight Diffraction Data from Liquid and Amorphous Samples*; Report RAL 89-046; Rutherford Appleton Laboratory: Chilton, Didcot, Oxon, U.K., 1989.
(18) Soper, A. K.; Luzar, A. *J. Chem. Phys.* **1992**, *97*, 1320.
(19) Soper, A. K. *Chem. Phys.* **1996**, *202*, 298.
(20) Soper, A. K. *Phys. Rev. B* **2005**, *72*, 104204.
(21) Soper, A. K. *Mol. Phys.* **2001**, *99*, 1503.
(22) Bowron, D. T.; Finney J. L.; Soper, A. K. *J. Am. Chem. Soc*. **2006**, *128*, 5119.
(23) Soper, A. K. *Chem. Phys.* **2000**, *258*, 121.
(24) Soper, A. K.; Ricci, M.-A. *Phys. Rev. Lett.* **2000**, *84*, 2881.
(25) Finney, J. L.; Bowron, D. T.; Soper, A. K.; Loerting, T.; Mayer, E.; Hallbrucker, A. *Phys. Rev. Lett.* **2002**, *89*, 205503.
(26) Finney, J. L.; Hallbrucker, A.; Kohl, I.; Soper, A. K.; Bowron, D. T. *Phys. Rev. Lett.* **2002**, *88*, 225503.
(27) Svishchev, I. M.; Kusalik, P. G. *J. Chem. Phys.* **2002**, *99*, 3049.
(28) Soper, A. K. *J. Chem. Phys.* **1994**, *101*, 6888.
(29) Bedard-Hearn, M. J.; Larsen, R. E.; Schwartz, B. J. *J. Chem. Phys.* **2005**, *122*, 134506.
(30) Martini, I. B.; Barthel, E. R.; Schwartz, B. J. *Science* **2001**, *293*, 462.